CELLULASE 6 and MANNANASE 7 affect cell differentiation and silique dehiscence in Arabidopsis

Hanjun He,[a,b] Mei Bai,[a] Yanting Hu,[a] Hong Wu,[a] and Ming Yang[b]

[a] State Key Laboratory for Conservation and Utilization of Subtropical Agro-bioresources, South China Agricultural University, Guangzhou, China.

[b] Department of Plant Biology, Ecology, and Evolution, Oklahoma State University, Stillwater, OK, USA

ABSTRACT

Cellulases, hemicellulases and pectinases play important roles in fruit development and maturation, but mutants with defects in the fruit have not been reported for cellulase or hemicellulase genes. Here we report the functional characterization of cellulase gene *CEL6* and hemicellulase gene *MAN7* in silique development and dehiscence in Arabidopsis. These genes were found to be expressed in vegetative and reproductive organs, and their expression in the silique partially depended on the IND and ALC transcriptional factors. Mutant alleles of *cel6* and *man7* exhibited delayed secondary cell wall thickening and altered cell morphology in the valve margin and impaired silique dehiscence. Cells in the separation layer in nearly mature siliques of the single mutants and the *cel6-1 man7-3* double mutant remained intact whereas they degenerated in the wild-type control. Phenotypic studies of single, double, triple and quadruple mutants revealed that the higher-order mutant combinations of the *cel6-1*, *man7-3*, and pectinase *adpg1-1 and adpg2-1* mutations produced more severe silique indehiscent phenotypes than the corresponding lower-order mutant combinations, except for some combinations involving *cel6-1*, *man7-3*, and *adpg2-1*. Our results demonstrate that the ability of the silique to dehisce can be manipulated to different degrees by altering the activities of proteins of different types.

INTRODUCTION

Cellulases, hemicellulases, and pectinases are the three types of cell wall-degrading enzymes that function in cell differentiation, abscission, and dehiscence in plants. Although the biochemical reactions involving these enzymes are generally understood, genetic studies of a combined effect of loss of function in more than one type of these enzymes on a plant developmental process have not been conducted. Such studies can yield insight into how the three types of enzymes together affect the same plant developmental process, which may be relevant to improving agriculturally important traits of crops.

RESULTS

CEL6 and *MAN7* are expressed in the silique and their expression is partially dependent on IND and ALC (Figs. 1 and 3)

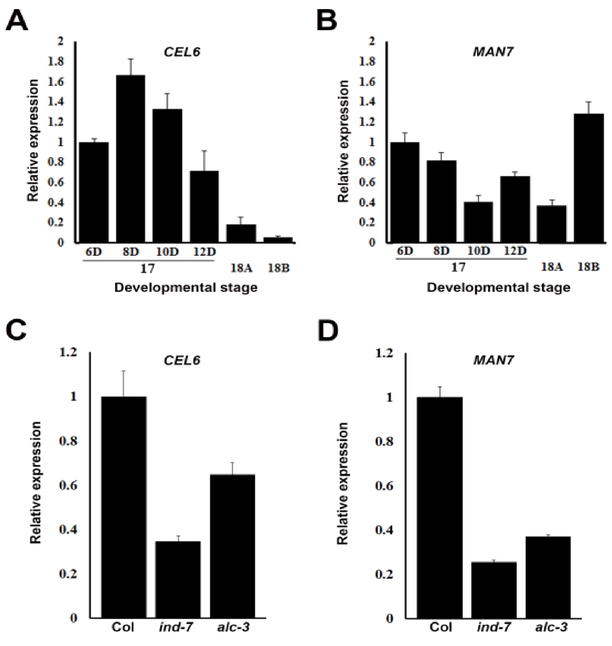

Figure 1. RT-qPCR results of the CEL6 and MAN7 genes in siliques of Col-0 and the *ind-7* and *alc-3* mutants.

(A) CEL6 expression at different developmental stages of Col-0.
(B) MAN7 expression at different developmental stages of Col-0.
(C) CEL6 expression at stage 17B in Col-0 and the *ind-7*, and *alc-3* mutant.
(D) MAN7 expression at stage 17B in Col-0 and the *ind-7*, and *alc-3* mutant.
6D-12D in (A) and (B) are days after anthesis. Shown in each plot are average relative expression levels with the value of the first bar on the left being 1.

Expression of *CEL6* and *MAN7* is reduced in late silique development in *ind-7* and *alc-3*

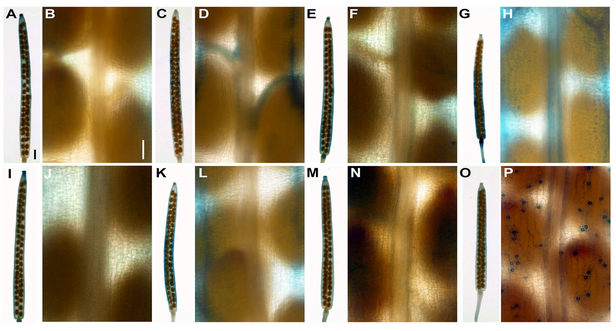

Figure 3. GUS-signals from *pCEL6:GUS* and *pMAN7:GUS* in siliques of the *ind-7* and *alc-3* mutants.

(A-F) pCEL6:GUS in the *ind-7* mutant.
(G-L) pCEL6:GUS in the *alc-3* mutant.
(M-R) pMAN7:GUS in the *ind-7* mutant.
(S-X) pMAN7:GUS in the *alc-3* mutant.
Siliques in (A), (E), (I), and (M) were at stage 17, and in (C), (G), (K), and (O) at stage 18. (B), (D), (F), (H), (J), (L), (N), and (P) are a higher magnification of the siliques to their immediate left, respectively. Bar in (A) = 1 mm for (A), (C), (E), (G), (I), (K), (M), and (O), and in (B) = 100 µm for (B), (D), (F), (H), (J), (L), (N), and (P).

Expression domains of *CEL6* and *MAN7* largely overlap in vegetative (not shown) and reproductive organs (Fig. 2)

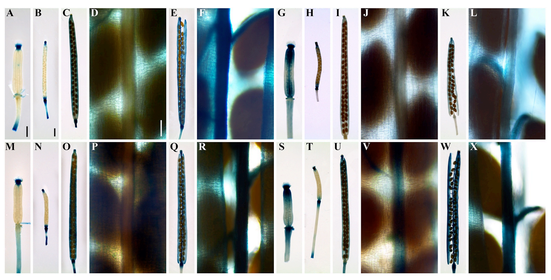

Figure 2. GUS-staining patterns in siliques of the GUS-promoter and GUS-protein fusion lines of the CEL6 and MAN7 genes.

(A-F) Siliques of a pCEL6:GUS line.
(G-L) Siliques of a pMAN7:GUS line.
(M-R) Siliques of a pCEL6:CEL6-GUS line.
(S-X) Siliques of a pMAN7:MAN7-GUS line.
Siliques in (A), (G), (M), and (S) were at stage 15, in (B), (H), (N), and (T) at stage 16, in (C), (D), (I), (J), (O), (P), (U), and (V) at stage 17, and in (E), (F), (K), (L), (Q), (R), (W), and (X) at stage 18. (D), (F), (J), (L), (P), (R), (V), and (X) are higher magnifications of the siliques to their immediate left, respectively. Bar in (A) = 500 µm for (A), (G), (M), and (S), in (B) = 1 mm for (B), (C), (E), (H), (I), (K), (N), (O), (Q), (T), (U), and (W), and in (D) = 100 µm for (D), (F), (J), (L), (P), (R), (V), and (X).

Overexpression of *CEL6* and *MAN7* moderately promotes silique dehiscence (Fig. 8)

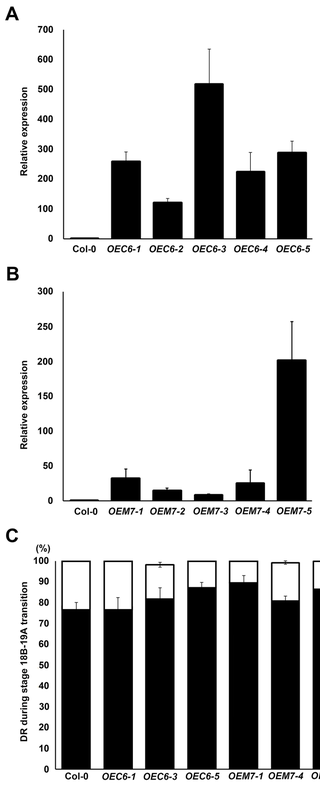

Figure 8. RT-qPCR results and silique dehiscence rates of *CEL6*- and *MAN7*-overexpression lines.

(A) Average relative expression levels (± standard errors) of *CEL6* in stage-17B siliques in Col-0 and five *CEL6*-overexpression lines (*OEC6-1 to OEC6-5*). The level in Col-0 is defined as 1.
(B) Average relative expression levels (± standard errors) of *MAN7* in stage-17B siliques in Col-0 and five *MAN7*-overexpression lines (*OEM7-1 to OEM7-5*). The level in Col-0 is defined as 1.
(C) Average dehiscence rates (± standard errors) of two consecutive siliques during the stage 18B-19A transition. Black bars are of the younger siliques and open bars of the older siliques. DR-average dehiscence rate.

The *cel6* and *man7* mutants are defective in cell differentiation in the valve margin and impaired in silique dehiscence (Figs. 4-7)

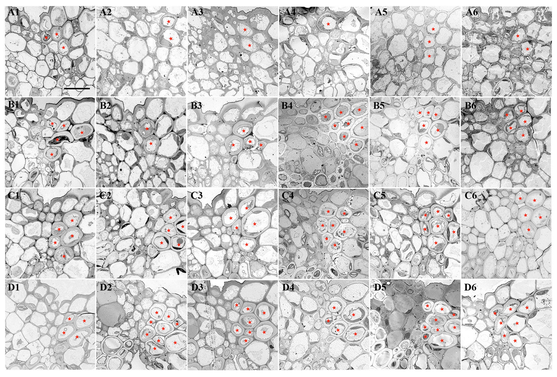

Figure 5. Transmission electron microscopy images of transverse sections of stage-17 siliques of Col-0 and the *cel6* and *man7* mutants.

(A1), (B1), (C1), and (D1) Col-0.
(A2), (B2), (C2), and (D2) The *cel6-1* mutant.
(A3), (B3), (C3), and (D3) The *cel6-2* mutant.
(A4), (B4), (C4), and (D4) The *man7-1* mutant.
(A5), (B5), (C5), and (D5) The *man7-3* mutant.
(A6), (B6), (C6), and (D6) The *cel6-1 man7-3* double mutant.
(A1-6) Siliques at the stage of 4D (4 days after anthesis).
(B1-6) Siliques at the stage of 6D.
(C1-6) Siliques at the stage of 8D.
(D1-6) Siliques at the stage of 10D.
Red stars in Col-0 indicate lignified cells, and in the mutants either cells presumably to be lignified or lignified cells, in the dehiscence zoon.
Bar = 10 µm for all the images.

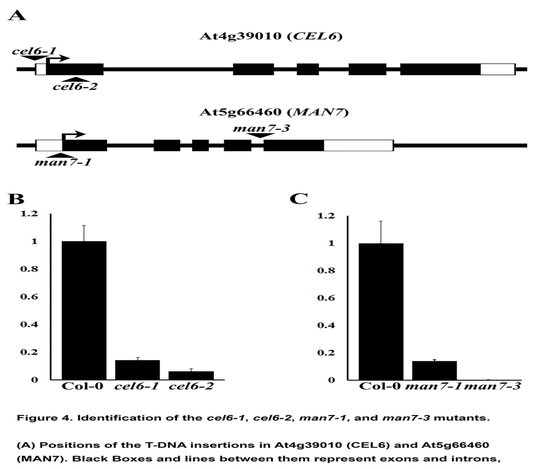

Figure 4. Identification of the *cel6-1*, *cel6-2*, *man7-1*, and *man7-3* mutants.

(A) Positions of the T-DNA insertions in At4g39010 (CEL6) and At5g66460 (MAN7). Black Boxes and lines between them represent exons and introns, respectively. Open boxes represent the predicted 5'- and 3'-untranslated regions. Triangles indicate the positions of the T-DNA insertions.
(B) Average relative expression levels (± standard errors) of *CEL6* in stage-17 siliques of Col-0 and the *cel6-1*, and *cel6-2* mutants. The Col-0 expression level is defined as 1.
(C) Average relative expression levels (± standard errors) of *MAN7* in stage-17 siliques of Col-0 and the *man7-1*, and *man7-3* mutants. The Col-0 expression level is defined as 1.

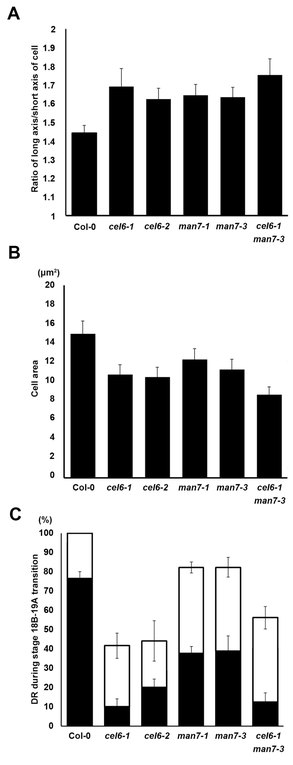

Figure 7. Silique phenotypes in Col-0 and the *cel6* and *man7* mutants.

(A) Average ratios (± standard errors) of long axis to short axis of cells in the separation layer.
(B) Average cell areas (± standard errors) of cells in the separation layer.
(C) Average dehiscence rates (± standard errors) of two consecutive siliques during the stage 18B-19A transition. Black bars are of the younger siliques and open bars of the older siliques. DR-average dehiscence rate.

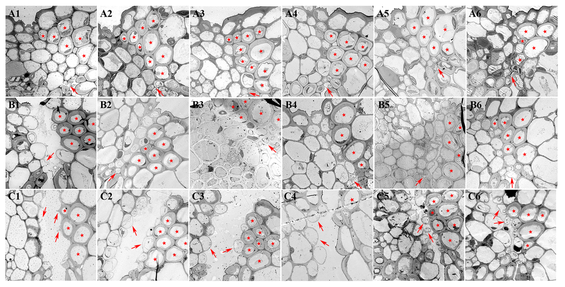

Figure 6. Transmission electron microscopy images of transverse sections of stage-17B-to-stage-18 siliques of Col-0 and the *cel6* and *man7* mutants.

(A1), (B1), and (C1) Col-0.
(A2), (B2), and (C2) The *cel6-1* mutant.
(A3), (B3), and (C3) The *cel6-2* mutant.
(A4), (B4), and (C4) The *man7-1* mutant.
(A5), (B5), and (C5) The *man7-3* mutant.
(A6), (B6), and (C6) The *cel6-1 man7-3* double mutant.
(A1-6) Siliques at stage 17B (12D).
(B1-6) Siliques at stage 18A.
(C1-6) Siliques at stage 18B.
Red stars indicate lignified cells in the dehiscence zoon. Arrows indicated degenerating cells or cell wall stubs from degenerated cells of the separation layer in Col-0, or intact cells of the separation layer in the mutants. Bar = 10 µm for all the images.

The silique indehiscent phenotypes of *adpg1-1* and *adpg1-1 adpg2-1* are enhanced by the *cel6-1* and *man7-3* mutations (Figs. 9-10)

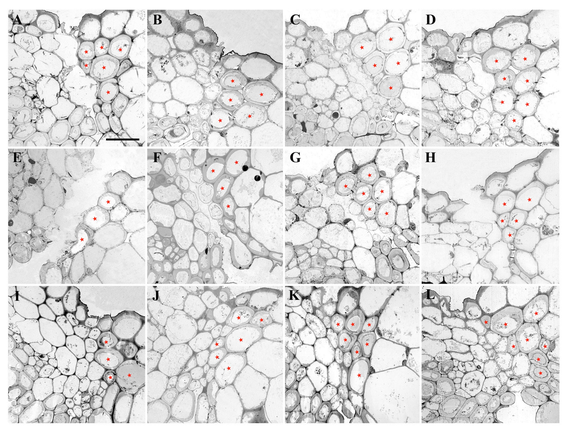

Figure 9. Transmission electron microscopy images of transverse sections of stage-18B siliques in single, double, triple, and quadruple mutants.

(A) The *adpg1-1* mutant.
(B) The *cel6-1 adpg1-1* double mutant.
(C) The *man7-3 adpg1-1* double mutant.
(D) The *cel6-1 man7-3 adpg1-1* triple mutant.
(E) The *adpg2-1* mutant.
(F) The *cel6-1 adpg2-1* double mutant.
(G) The *man7-3 adpg2-1* double mutant.
(H) The *cel6-1 man7-3 adpg2-1* triple mutant.
(I) The *adpg1-1 adpg2-1* double mutant.
(J) The *cel6-1 adpg1-1 adpg2-1* triple mutant.
(K) The *man7-3 adpg1-1 adpg2-1* triple mutant.
(L) The *cel6-1 man7-3 adpg1-1 adpg2-1* quadruple mutant.
Red stars indicate lignified cells in the dehiscence zoon. Bar = 10 µm for all images.

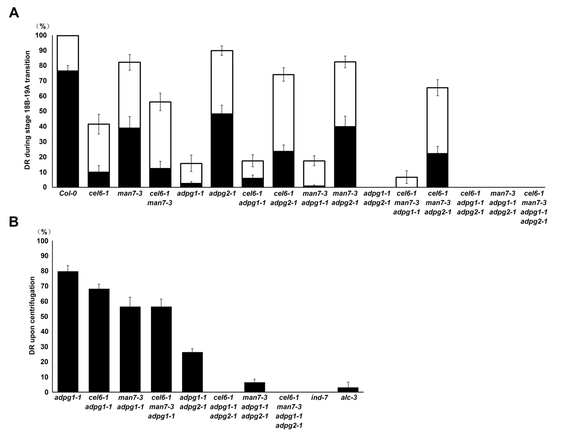

Figure 10. Average dehiscence rates (± standard errors) in the single, double, triple, and quadruple mutants.

(A) During the stage 18B-19A transition. Black bars are of the younger siliques and open bars of the older siliques.
(B) Stage-19A siliques of naturally indehiscent or nearly indehiscent genotypes after the centrifugation impact.
DR-average dehiscence rate.

CONCLUSIONS

CEL6 and MAN7 affect cell differentiation in the silique and contribute to silique dehiscence. The ability of the silique to dehisce is differentially affected by the loss of function in the number and types of genes involved in the process.